Scientia Iranica, Vol. 10, No. 4, pp 373-382

SCIENTIA
IRANICA

Optical Band Gap Studies of Tungsten Sulphoselenide Single Crystals Grown by a DVT Technique

D.A. Dholakia[1], G.K. Solanki*, S.G. Patel[1] and M.K. Agarwal[1]

In this paper, the optical absorption edge was measured on basal plane samples of DVT grown single crystals of WS_xSe_{2-x} ($0 \leq x \leq 2$) at room temperature. The incident light beam was kept normal to the basal plane, i.e. along the c-axis of the grown flakes. Results were analyzed on the basis of two- and three-dimensional models. It was observed that both direct and indirect symmetry allowed transitions to give a good account of the absorption edge in WS_xSe_{2-x}. The energy gaps and phonon energies were determined. The band gap varied smoothly with x, indicating that the band edges were the same for WSe_2, WS_2 and the other compounds of intermediate composition. The two-dimensional model results were similar to those obtained from the three-dimensional model and could, thus, be used to describe the main optical properties of WS_xSe_{2-x} single crystals.

INTRODUCTION

Following the energy crisis in the early 1970s, considerable effort was expended in the investigation of new semiconductors for interfacial solar energy conversion devices [1-5]. The semiconducting layered metal chalcogenides form a major class of new materials that have been investigated for energy conversion in photoelectrochemical (PEC) cells and in solid state (p-n Schottky) solar cells. However, the layered compounds have not yet found large-scale application in electronic devices. This is due to the fact that only limited materials research has been done in relation to the device potential of the layered semiconductors. On the other hand, they are quite promising and the studies reported so far, though exploratory in nature, serve to bring out the potential of these materials for photoelectronic devices.

The need to develop highly efficient and low cost techniques for solar energy conversion applications in solid state solar cells and in PEC cells is well recognized and has been adequately emphasized in various reviews and books [6]. The search for new materials has led to the synthesis and study of several novel layered semiconductors. Significant efforts have been made to produce defect free single crystals and high quality thin films of layered materials.

The layered transition metal dichalcogenides (TMDCs) are the most widely investigated of the layered materials with regard to their electronic properties. The TMDCs are very interesting solids since they display the whole spectrum of electronic properties covering insulators, semiconductors, nonmetals and superconductors [7-9]. Such a variation in the electronic behavior of the transition metal dichalcogenides is mainly due to the d-character of the valence and conduction bands that are derived from the nonbonding d-states of the transition metal.

Further, among TMDCs, layered structures of tungsten dichalcogenides (WSe_2 and WS_2) have been widely investigated. The attractive properties of these materials include the band gap in the region of optical solar energy conversion efficiency, anisotropy in their electrical behavior and stability against photoconversion reaction. Values up to 17% [10] and 22% [11] efficiency in energy conversion have been reported for single crystals of n-WSe_2 photoelectrodes, but more common values vary between 8 and 10%.

From the variation of solar energy conversion efficiency versus the band gap, Eg, and from literature it is found that the most promising material is one which has a band gap of $\sim$ 1.3 – 1.5 eV [12]. The

1. *Department of Physics, Sardar Patel University, Vallabh Vidyanagar - 388 120 Gujarat, India.*
*. *Corresponding Author, Department of Physics, Sardar Patel University, Vallabh Vidyanagar - 388 120 Gujarat, India.*

Table 1. Growth parameters used to synthesize single crystals of WS_xSe_{2-x}.

Crystal	Reaction Temperature (°C)	Growth Temperature (°C)	Growth Time (hr)	Crystal Size $(mm)^3$	Appearance
WSe_2	750	950	240	$19 \times 10 \times 0.26$	Black opaque
$WS_{0.5}Se_{1.5}$	770	980	240	$17 \times 7 \times 0.22$	Black opaque
WSSe	800	1010	240	$10 \times 8 \times 0.12$	Black opaque
$WS_{1.5}Se_{0.5}$	820	1040	240	$22 \times 6 \times 0.08$	Black opaque
WS_2	850	1080	240	$12 \times 10 \times 0.04$	Black opaque

direct energy gap for WSe_2 is 1.37 eV [13] and for WS_2 is 1.80 ± 0.03 eV [14]. It will, therefore, be highly desirable to synthesize mixed crystals of WS_2 and WSe_2, i.e. WS_xSe_{2-x}, and see how the band gap can be altered by varying the amount of sulphur and selenium in these mixed crystals of tungsten sulphoselenides. Hence, by synthesizing the entire series of WS_xSe_{2-x} with different values of 'x', one can prepare a material of optimum band gap for solar energy conversion.

In this work, considering tremendous potential of WS_xSe_{2-x}, authors have concentrated on the optical band gap measurement in WS_xSe_{2-x} for $x = 0$, 0.5, 1.0, 1.5 and 2.0. This study will be of immense help in the selection of an optimum material for PEC solar cell fabrication.

EXPERIMENTAL

Growth of Crystals

Single crystals of WS_xSe_{2-x} were grown using a direct vapor transport technique. In this technique, a stoichiometric mixture of W [99.95%], S [99.999%] and Se [99.99%] purity was loaded into a high quality fused quartz ampoule, which was sealed at a pressure of 10^{-5} torr. The sealed ampoule was then introduced into a two-zone furnace at a constant reaction temperature to obtain the charge of WS_xSe_{2-x}. The charge so prepared was rigorously shaken to ensure proper mixing of the constituents and kept in the furnace under appropriate conditions to obtain single crystals of WS_xSe_{2-x}. The growth conditions used for the synthesis are given in Table 1.

Crystal Structure

WS_xSe_{2-x} single crystals possess MoS_2 (C-7 type) layered crystal structure. The basic coordination unit for the tungsten in these layered structures is trigonal prismatic.

The structural unit of WS_xSe_{2-x} is a sandwich of three planes S/Se-W-S/Se. A S/Se-W-S/Se sandwich layer is composed of alternately occupied face centered prisms. No strong bond exists between the layers, only weak van der Waals forces hold the atomic sandwiches together. This gives the crystals their platy habit characteristic, with extended growth and pronounced cleavage perpendicular to the c-axis.

The structural data and X-ray density of single crystals of the series WS_xSe_{2-x} for $(0 \leq x \leq 2)$ as determined from X-ray diffraction are given in Table 2.

Table 2. Structural data and X-ray density of WS_xSe_{2-x}.

Crystal	Lattice Parameters			X-ray Density $(gm\ cm^{-3})$
	a (A°)	c (A°)	c/a	
WSe_2	3.298 ± 0.034	12.986 ± 0.026	3.938 ± 0.047	9.28
$WS_{0.5}Se_{1.5}$	3.270 ± 0.017	12.811 ± 0.047	3.919 ± 0.028	8.92
WSSe	3.229 ± 0.020	12.707 ± 0.035	3.936 ± 0.038	8.54
$WS_{1.5}Se_{0.5}$	3.201 ± 0.021	12.493 ± 0.068	3.904 ± 0.030	8.13
WS_2	3.178 ± 0.022	12.362 ± 0.003	3.890 ± 0.025	7.62

Use of UV-VIS-NIR Spectrophotometer for Obtaining the Absorption Spectra of WS_xSe_{2-x}

Grown crystals exhibit p-type conductivity with carrier concentrations of about $10^{16} - 10^{17}cm^{-3}$. For absorption measurements, thin samples were selected from grown in the form of thin flakes directly over the distributed charge. The a-axis and b-axis were contained in the plane of cleavage, i.e., along the basal plane. The absorption spectra were obtained by using a DK-2A spectrophotometer. Crystal flakes were pasted on a thick black paper with a cut exposing the crystal flake to the incident light. The reference used was a replica of the black paper, having the cut in exactly the same position as the crystal flake. This arrangement was necessary because the crystal size was smaller than that of the sample compartment. All samples of WS_xSe_{2-x} used in the present work since were in the form of thin platelets, as grown samples could be directly used to obtain their absorption spectra.

The thickness of the samples was measured by a micrometer or optical microscope. The absorption spectra were obtained in the range of 350 nm to 1450 nm. Thin crystals with thickness of about 0.0035 cm were used. All measurements were performed at room temperature with the incident beam normal to the basal plane, i.e. along the c-axis of the grown flakes. Measurements along the c-axis could not be performed since the specimens were too thin to be mounted along this direction.

ENERGY GAP DETERMINATION

The dependence of the absorption coefficient 'α' in terms of the direct and indirect transitions is most often performed with the help of the formulae derived for three-dimensional (3D) crystals. Their simplest form is as follows [15]:

$$(\alpha h\nu) = A(h\nu - E_g)^r, \tag{1}$$

for the direct transitions and:

$$(\alpha h\nu) = \sum_j B_j(h\nu - E_g' \pm E_{pj})^r, \tag{2}$$

for indirect transitions.

Here, α is the absorption coefficient, $h\nu$ the energy of the incident photon, E_g the energy for the direct transition, E_g' the energy for the indirect transition, E_{pj} the energies of the phonons assisting at indirect transitions, A and B are parameters depending in a more complicated way on temperature, phonon energy and photon energies E_p. However, for the analysis of the experimental results obtained at constant temperature, Equations 1 and 2 are sufficient and they are most often used while interpreting results on the absorption spectra obtained from semiconducting materials. The exponent r in the above equations depends upon whether the transition is symmetry allowed or not and the constants A and B assume different values for the allowed and forbidden transitions. For indirect transitions, the detailed form of Equation 2 [16-18] is given as:

$$\alpha_i = \sum_{i=1}^{2}\left\{\frac{B_{ai}}{E}\left(\frac{1}{e^{\frac{\theta_+}{T}}-1}\right)(E - E_g' + k\theta_i)^r + \frac{B_{ei}}{E}\left(\frac{1}{1-e^{-\theta_i/T}}\right)(E - E_g' - k\theta_i)^r\right\}, \tag{3}$$

where B_{ai} and B_{ei} are coefficients associated with absorption and emission of the ith phonon, E is the photon energy, E_g' the indirect energy gap and θ_i the phonon equivalent temperature defined by the following equation:

$$E_{pi} = k\theta_i, \tag{4}$$

where E_{pi} is the ith phonon energy. The use of Equations 1 to 3 for analyzing the absorption spectra is valid for semiconductors having a three-dimensional structure, but for anisotropic layered materials, one has to assume a two-dimensional form of the density of states [19]. In these cases, the density of states is a constant independent of the energy and the expressions showing the dependence of α in terms of direct and indirect transitions get modified as [20]:

$$\alpha = A'(h\nu - E_g)^r, \tag{5}$$

for direct transition and:

$$\alpha_i = \sum_{i=1}^{2}\left\{B_{ai}'\left(\frac{1}{e^{\frac{\theta_+}{T}}-1}\right)(E - E_g' + k\theta_i)^r + B_{ei}'\left(\frac{1}{1-e^{-\theta_i/T}}\right)(E - E_g' - k\theta_i)^r\right\}, \tag{6}$$

for indirect transitions [21].

The symbols in Equations 5 and 6 have the same meaning as explained earlier in [1-4]. Again, the exponent r depends on the dimensionality of the bands and whether the transitions are symmetry allowed or forbidden. Once again the coefficients A', B_{ai}' and B_{ei}' will be different for symmetry allowed and forbidden transitions. Possible values of r are given in Table 3 [13,19,20].

By plotting graphs of $(\alpha h\nu)^{1/r}$ against $h\nu$ for various values of r given in Table 3, it is possible to determine which of the conditions given in the table dominates. Extrapolations of these plots to zero absorption will provide the appropriate values of the energy gaps of the tungsten sulphoselenide compounds.

Table 3. Values of exponent 'r' for different types of band gap transitions.

Type of Transition	Direct		Indirect	
	Two-Dimensional	Three-Dimensional	Two-Dimentional	Three-Dimentional
Allowed	0 (Step function)	1/2	1	2
Forbidden	1	3/2	2	3

RESULTS

The absorption spectrum taken from a WSSe single crystal in the form of a thin flake over the spectral range of 700 nm to 1450 nm is shown in Figure 1.

A careful study of this spectrum reveals that an absorption edge is seen in the spectral range of 700 nm to 850 nm. In order to analyze the results obtained from this spectrum in the vicinity of the absorption edge on the basis of two as well as three-dimensional models, values of absorption coefficient 'α' were determined at every step of 2.5 nm. The interpretation of the results in the terms of direct and indirect transitions can be performed with the help of Equations 1, 3, 5 and 6 using the various values of 'r' from Table 3. Figure 2 shows the spectral variation of $(\alpha h\nu)^{1/2}$ vs $h\nu$. Since the curve indicates a discontinuous straight line, it is quite plausible that it represents indirect interband transitions, involving the emission or absorption of phonons. In order to make an accurate determination of the points of discontinuities, authors have followed the method adopted by Koshkin et al. [22] and Elkorashy [18].

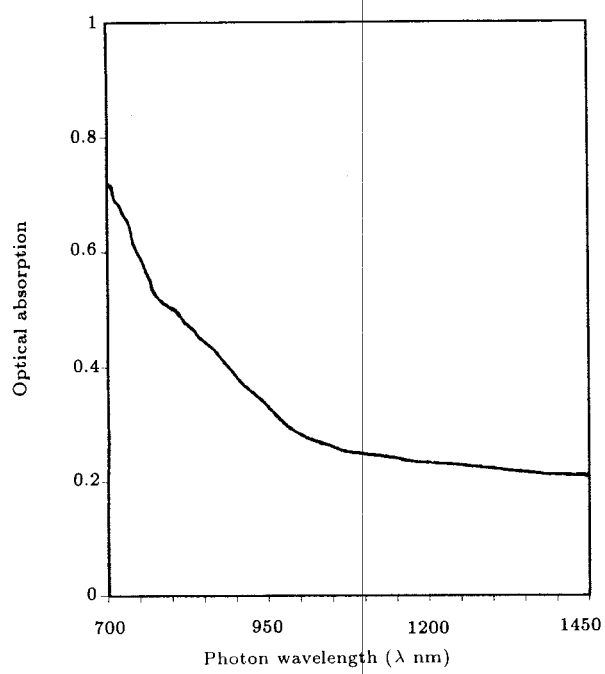

Figure 1. Absorption spectrum from a single crystal of WSSe.

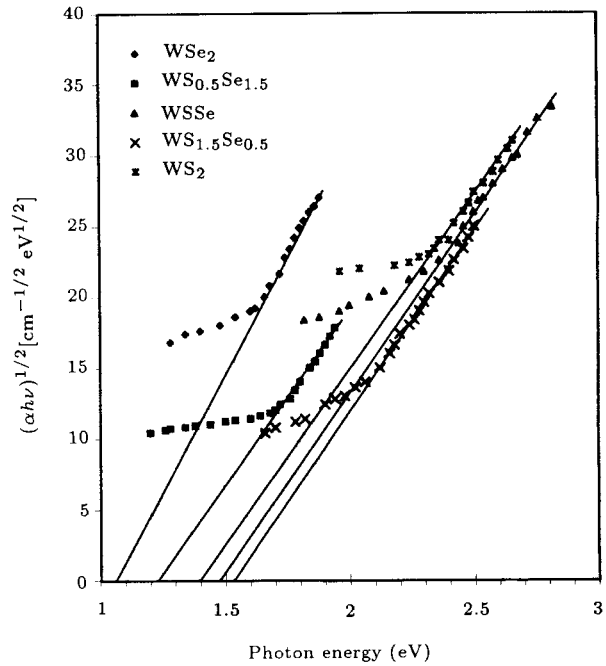

Figure 2. $(\alpha h\nu)^{1/2}$ vs photon energy for the series WS_xSe_{2-x}.

Accordingly, from the graphical differentiation of the data presented in Figure 2, the dependence of the derivatives $\delta(\alpha h\nu)^{1/2}/\delta(h\nu)$ on $h\nu$ has been shown in Figure 3. It can be clearly seen, from this figure, that the derivatives are step functions of energy with four steps well defined in the range of $E_1 < E < E_2$, $E_2 < E < E_3$, $E_3 < E < E_4$ and $E_4 < E$.

The values of E_1, E_2, E_3 and E_4 indicate the points of discontinuities in the plot of $\delta(\alpha h\nu)^{1/2}/\delta h\nu$ vs $h\nu$. The indirect energy gaps obtained from these values of E_1, E_2, E_3 and E_4 are given by:

$$E_g' = \frac{E_1 + E_4}{2} = \frac{E_2 + E_3}{2}, \tag{7}$$

and the phonon energies are given by:

$$E_{P1} = \frac{E_4 - E_1}{2} \quad \text{and} \quad E_{p2} = \frac{E_3 - E_2}{2}.$$

The values of indirect band gap E_g' and phonon energies thus obtained are given in Table 4. The value of E_g' can also be obtained from the intersection of the linear portion of the graph in Figure 2 with the energy

Table 4. Indirect energy gaps and phonon energies of WS_xSe_{2-x} for $x = 0, 0.5, 1.0, 1.5$ and 2.0.

	Three-Dimensional Model					Two-Dimensional Model				
	WSe_2	$WS_{0.5}Se_{1.5}$	WSSe	$WS_{1.5}Se_{0.5}$	WS_2	WSe_2	$WS_{0.5}Se_{1.5}$	WSSe	$WS_{1.5}Se_{0.5}$	WS_2
E_1(eV)	1.02	1.16	1.355	1.47	1.50	1.04	1.18	1.28	1.39	1.45
E_2(eV)	1.06	1.19	1.374	1.48	1.51	1.06	1.20	1.32	1.42	1.49
E_3(eV)	1.09	1.22	1.393	1.49	1.53	1.09	1.23	1.35	1.45	1.52
E_4(eV)	1.13	1.25	1.405	1.50	1.55	1.11	1.25	1.39	1.48	1.56
E'_g(C)	1.08	1.21	1.38	1.48	1.52	1.08	1.22	1.34	1.44	1.51
E'_g(E)	1.05	1.22	1.38	1.48	1.52	1.08	1.22	1.34	1.44	1.51
E_{p1}(meV)	57.14	42.65	24.89	15.56	23.41	37.50	38.90	52.39	43.80	57.76
E_{p2}(meV)	18.81	14.72	9.62	6.67	9.36	14.92	16.47	14.46	14.59	16.06

E'_g (C): Indirect band gap from calculation,

E'_g (E): Indirect band gap from extrapolation.

axis for zero absorption. This value closely matches the value obtained from Equation 4.

Further, a graph of $(\alpha h\nu)^{1/3}$ vs $h\nu$ representing the indirect forbidden transition (Table 3) is shown in Figure 4. The intersection of the straight-line portion of this graph with the energy axis for zero absorption gives unacceptably low values for the indirect band gap E'_g. Moreover a graphical differentiation of the data presented in this figure and the intersection of the straight line portion of the graph with the energy axis for zero absorption will give widely different values. It is, therefore, conjectured that the indirect transition represented by the absorption curve is an indirect allowed type.

In order to analyze the data from the absorption curve on the basis of the two-dimensional model, a variation of α vs $h\nu$ was studied. A graph showing the spectral variation of α is shown in Figure 5. A graphical differentiation of the data presented in this figure is shown in Figure 6.

The value of indirect band gap E'_g obtained from the extrapolation of the linear portion of the curve in Figure 5 and that obtained from the graphical differentiation of the data in Figure 6, are shown in Table 4. The values of phonon energies obtained from Figure 6 are also given in this table. From Table 4, it is clearly evident that the optical energy gap in WSSe is indirect allowed with absorption and emission of the phonons with energies of 24.89 and 9.62 meV, respectively. The results obtained from the three-dimensional analysis are also confirmed by two-dimensional analysis of the data.

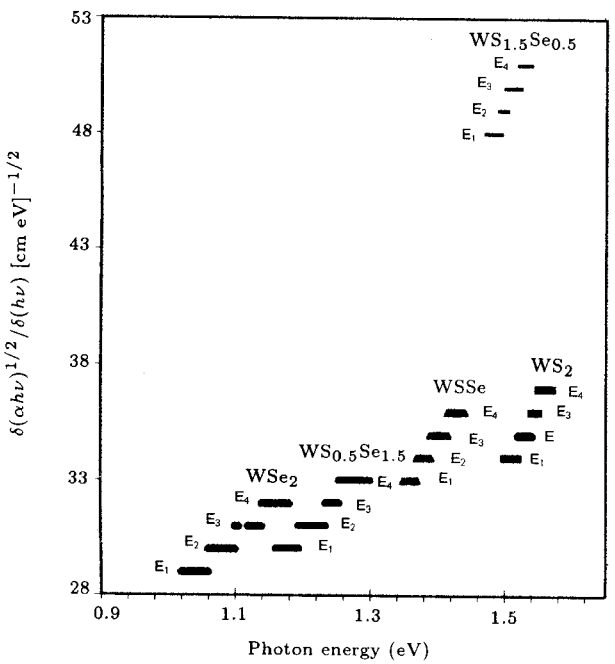

Figure 3. The spectral variation of the derivative $\delta(\alpha h\nu)^{1/2}/\delta(h\nu)$ obtained by graphical differentiation of the data presented in Figure 2.

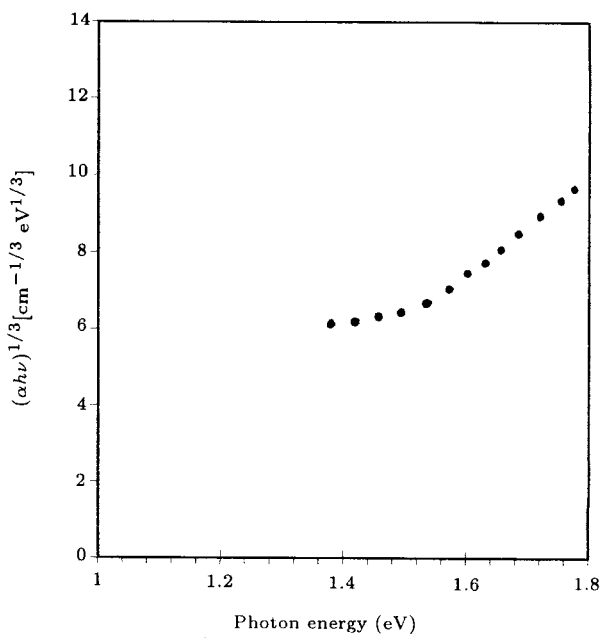

Figure 4. $(\alpha h\nu)^{1/3}$ vs photon energy for WSSe single crystal.

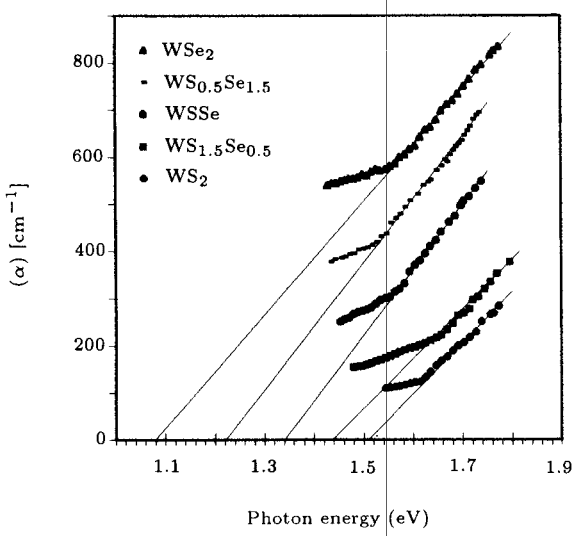

Figure 5. (α) vs photon energy for the series WS_xSe_{2-x}

Taking the values of E_g' and E_{pl} at room temperature from Table 4, the constants B_{a1}, B_{a2}, B_{e1}, B_{e2}, θ_1 and θ_2 appearing in Equation 2 and similar constants $B'_{a1}, B'_{a2}, B'_{e1}, B'_{e2}, \theta_1$ and θ_2 appearing in Equation 6 have been determined with the help of Equations 2 and 6 taking the value of r for the three- and two-dimensional models from Table 3. All these values are presented in Table 5.

For the determination of the direct band gap, E_g on the basis of two-dimensional model, it is seen that Equation 5 (with the value of r from Table 3) takes the form:

$$\alpha = A'S(h\nu - E_g),$$

and:

$$\alpha = A'(h\nu - E_g),$$

for the allowed and forbidden type transitions, respectively, where A' is a constant and the step function $S(h\nu - E_g) = 1$ for $E > E_g$ and $S = 0$ for $E < E_g$. In absence of a discrete step in the absorption spectrum, our results cannot be fitted to an equation corresponding to a direct electronic transition on the basis of two-dimensional model. Therefore, according to 2D model, the experimental points in the present work could be best fitted to an equation, which corresponds to indirect electronic transitions.

Therefore, for the determination of direct band gap only 3D model was used. According to this model, taking the value of r corresponding to direct allowed transition from Table 3, the spectral variation of $(\alpha h\nu)^2$ vs $h\nu$, as shown in Figure 7, was studied.

The value of E_g obtained from the intercept of the straight line, portion of the curve on the $h\nu$ axis for zero absorption is shown in Table 6.

For finding the value of the direct band gap corresponding to direct forbidden transition on 3D model, the value of r was taken as 3/2 from Table 3. Accordingly, the variation of $(\alpha h\nu)^{2/3}$ vs $h\nu$ was considered. Since the intersection of the linear portion of this graph with $h\nu$ axis for zero absorption gave unacceptably low value for the direct band gap E_g, it

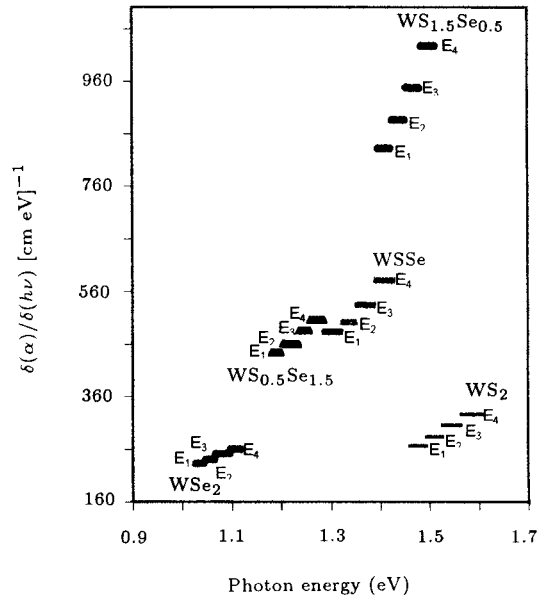

Figure 6. The spectral variation of the derivative $\delta(\alpha)/\delta(h\nu)$ obtained by graphical differentiation of the data presented in Figure 5.

Table 5. Constants of Equations 3 and 6.

Constant	Three-Dimensional Model					Constant	Two-Dimensional Model				
	WSe_2	$WS_{0.5}Se_{1.5}$	WSSe	$WS_{1.5}Se_{0.5}$	WS_2		WSe_2	$WS_{0.5}Se_{1.5}$	WSSe	$WS_{1.5}Se_{0.5}$	WS_2
$B_{e1}(cm^{-1}eV^{-2})$	18648.8	81391.1	744716.8	609776 .3	1246830.5	$B'_{e1}(cm^{-1}eV^{-2})$	2216.8	1029.6	1082.2	6068.8	1259.1
$B_{a1}(cm^{-1}eV^{-2})$	95808.7	197277.2	669156.7	2244745.0	7346683.0	B'_{a1} $(cm^{-1}eV^{-2})$	10643.6	7161.6	4527.3	3750.0	11433.3
$B_{e2}(cm^{-1}eV^{-2})$	26560.1	94402.5	1146876.2	1086184.6	3132951.3	B'_{e2} $(cm^{-1}eV^{-2})$	3382.5	1040.1	2813.4	4234.3	1364.1
$B_{a2}(cm^{-1}eV^{-2})$	45580.5	128502.2	1085374.6	1906508.6	6328467.7	B'_{a2} $(cm^{-1}eV^{-2})$	6295.7	2808.9	5104.2	7652.5	4577.8
θ_1(K)	662.58	494.59	288.61	180.46	271.46	θ_1(K)	434.78	451.01	607.47	507.88	611.78
θ_2(K)	218.16	170.77	111.58	71.33	108.57	θ_2(K)	172.98	191.06	167.65	169.15	186.20

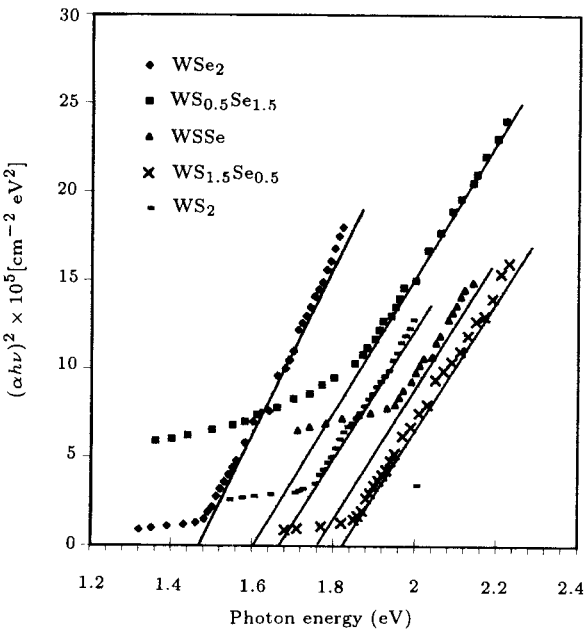

Figure 7. $(\alpha h\nu)^2$ vs photon energy for the series WS_xSe_{2-x}.

is conjectured that the direct transition represented by absorption curve is direct allowed.

In order to see the effect of making tungsten sulphoselenide rich in sulphur or selenium content on the absorption spectra of tungsten sulphoselenide (WSSe), the absorption spectra were obtained for WSe_2, $WS_{0.5}Se_{1.5}$, $WS_{1.5}Se_{0.5}$ and WS_2 in the spectral range of 700 nm to 1450 nm. Similar to WSSe values of 'α' were determined from the absorption spectra at every interval of 2.5 nm and the spectral variation of $(\alpha h\nu)^{1/2}$ for single crystals of WSe_2, $WS_{0.5}Se_{1.5}$, $WS_{1.5}Se_{0.5}$ and WS_2 is shown in Figure 2.

Graphical differentiation of the data presented in this figure was carried out and the graphs of $\delta(\alpha h\nu)^{1/2}/\delta h\nu$ vs $h\nu$ are shown in Figure 3.

In order to carry out the analysis represented in Figure 2, on the basis of the two-dimensional model, graphs of (α) vs $h\nu$ for WSe_2, $WS_{0.5}Se_{1.5}$, $WS_{1.5}Se_{0.5}$ and WS_2 are shown in Figure 5.

The graphical differentiation of the data in this figure is shown in Figure 6

The values of E_1, E_2, E_3 and E_4 indicating the points of discontinuities in Figure 2, the values of indirect band gap E'_g and the phonon energies E_{p1} and E_{p2} obtained in the manner similar to WSSe on the basis of the three-dimensional model are represented in Table 4.

The values of E_1, E_2, E_3, E_4, $E'_g(C)$ and $E'_g(E)$, the phonon energies E_{p1} and E_{p2} determined on the basis of the two-dimensional model are also shown in this table. The values of indirect band gaps obtained from the extrapolations of the straight line portions of the graphs in Figures 2 and 5 are also given in this table.

Taking the values of E'_g and E_{pl} for WSe_2, $WS_{0.5}Se_{1.5}$, $WS_{1.5}Se_{0.5}$ and WS_2 from Table 4, the constants $B_{a1}, B_{a2}, B_{e1}, B_{e2}, \theta_1$ and θ_2 on the basis of three dimensional model and constants $B'_{a1}, B'_{a2}, B'_{e1}, B'_{e2}, \theta_1$ and θ_2 on the basis of two-dimensional model for all these compounds were estimated as before and the results are represented in Table 5.

For the determination of the direct band gap for sulphur deficient (i.e. WSe_2, $WS_{0.5}Se_{1.5}$) and sulphur rich (i.e. $WS_{1.5}Se_{0.5}$, WS_2) compounds in WS_xSe_{2-x}, the best fit for all the experimental points was obtained in spectral variation of $(\alpha h\nu)^2$ for the case of three-dimensional model only. These curves for WSe_2, $WS_{0.5}Se_{1.5}$,$WS_{1.5}Se_{0.5}$ and WS_2 are shown in Figure 7.

The values of direct band gap E_g obtained by the extrapolation of the straight line portions in these curves on $h\nu$ axis for zero absorption are represented in Table 6.

DISCUSSION

It is quite clear from the analysis of the absorption data (based on three- as well as two-dimensional models) presented above that both direct and indirect symmetry allowed transitions give a good account of the absorption edge in WSSe and sulphur deficient (i.e. WSe_2, $WS_{0.5}Se_{1.5}$) and sulphur rich (i.e. $WS_{1.5}Se_{0.5}$, WS_2) compounds of tungsten sulphoselenide. The fact that analysis based on the two-dimensional model is also able to provide a consistent explanation supports the high anisotropic nature of these compounds and suggests that two-dimensional behavior seems likely for these compounds.

The values of direct and indirect band gaps for the end members of the series, i.e. WSe_2 and WS_2 agree with the results of earlier investigators shown in Table 7.

The values for the middle compounds $WS_{0.5}Se_{1.5}$, WSSe and $WS_{1.5}Se_{0.5}$ are reported for the first time,

Table 6. Direct energy gaps for WS_xSe_{2-x} single crystals.

Model	Value of E_g in eV				
	WSe_2	$WS_{0.5}Se_{1.5}$	WSSe	$WS_{1.5}Se_{0.5}$	WS_2
Three-dimensional	1.45	1.58	1.65	1.74	1.80

Table 7. Optical band gaps of WSe_2 and WS_2 obtained by different investigators.

Material	Direct Band Gap(E_g) eV	Indirect Band Gap(E'_g) eV	Investigators
WSe_2 (single crystal)	1.37	1.219	[13,23,24]
	1.55		[25]
		1.16	[26,27]
	1.57	1.40	[28,29]
	1.775		[30]
WSe_2 (thin film)	1.57	1.37	[31]
		0.98	[32]
WS_2 (single crystal)	1.78	1.34	[13,23,31,33,34]
	1.77		[29]
WS_2 (thin film)	1.89	1.29	[31]

since such a detailed study of the absorption spectra is not available in the literature. It has been conclusively shown that the estimates of the indirect band gaps obtained from the extrapolations of the $(\alpha h\nu)^{1/2}$ vs $h\nu$ and (α) vs $h\nu$ curves, with the zero absorption, match with those obtained from the graphical differentiation of the data.

A careful study of the data presented in Tables 4 and 6 indicates that both direct as well as indirect band gaps increase with an increase of sulphur content in WS_xSe_{2-x} single crystals. For direct band gaps in mixed III-V semiconducting materials, it is customary as shown by van Vechten and Bergstresser [35] to express the compositional dependent energy gap as:

$$E(x) = E(0) + bx + cx^2,$$

where c is called the bowing parameter. For direct and indirect band gaps in the present work, if $E(x)$ is fitted to this expression, the results shown in Table 8 will be obtained.

Figure 8 shows the dependence on x of the direct (E_g) and indirect (E'_g) band gaps, respectively, on the basis of the three-dimensional model. Similar dependence of E'_g on x on the basis of two-dimensional model is represented in Figure 9, respectively.

In these figures, optical direct and indirect band gaps of WS_xSe_{2-x} single crystals have been plotted against x at 300°K. The curves are least squares fit to:

$$E(x) = E(0) + bx + cx^2.$$

The change in energy gap, both direct as well as indirect, with respect to x is smooth. There are no abrupt slope changes indicating that a different

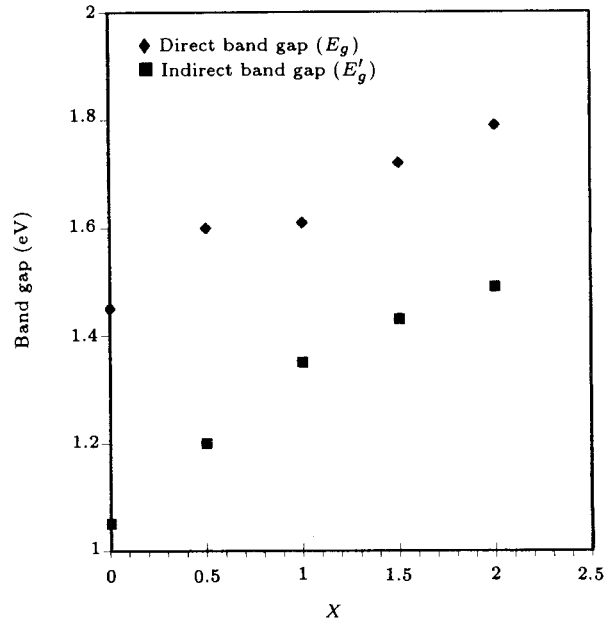

Figure 8. Graphs showing the dependence of the direct (E_g) and indirect (E'_g) band gaps on x in WS_xSe_{2-x} on the basis of three-dimensional model.

band maximum might be replacing that of WSe_2 as x increases. Thus, it can be concluded that the band edges are the same in all these compounds. There are no changes in the nature of the valence band maximum or conduction band minimum.

The increase in band gap with a rise of sulphur content can be linked with increasing resistivity with x, i.e. sulphur rich compounds in WS_xSe_{2-x} are more resistive compared to sulphur deficient ones. The ability to obtain a consistent analysis of the absorption data on the two-dimensional model suggests that the material tungsten sulphoselenide is highly anisotropic. The

Table 8. Band gaps of WS_xSe_{2-x} for various values of x. (least-squares fit to) $E(x) = E(0) + bx + cx^2$.

Model	Band Gap	T(K)	E_0(eV)	b(eV)	c(eV)
Three-dimensional	Direct (E_g)	300	1.44	0.256	-0.04
	Indirect (E'_g)	300	1.04	0.422	-0.09
Two-dimensionalø	Indirect (E'_g)	300	1.04	0.376	-0.07

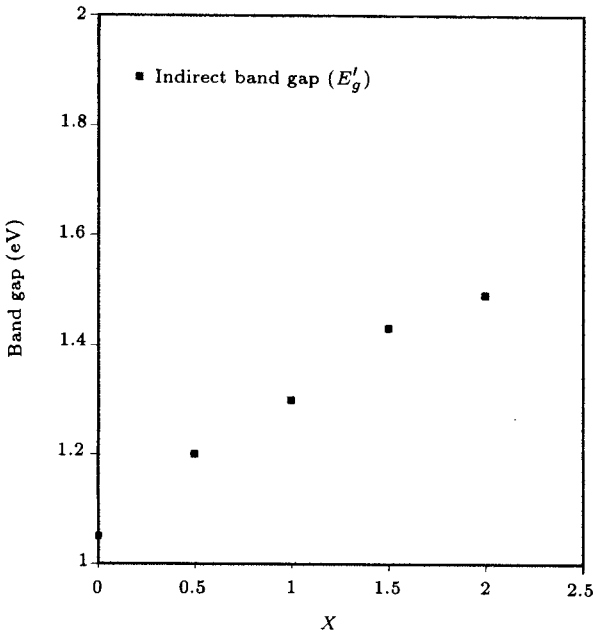

Figure 9. Graphs showing the dependence of the indirect (E_g') band gaps on x in WS_xSe_{2-x} on the basis of two-dimensional model.

fact that the three-dimensional model also provides an accurate analysis indicates the possibility of conduction along the c-axis because of the presence of stacking faults in these crystals.

ACKNOWLEDGMENT

The financial support provided by University Grants Commission (UGC), New Delhi for carrying out this research work is gratefully acknowledged.

REFERENCES

1. Pleskov, Y.V. "Solar energy congress", *A Photoelectrochemical Approach*, Springer Verlag, Berlin-Hiedelberg (1990).
2. Heller, A., Ed. "Semiconductor-liquid junction solar cells", *The Electrochemical Society*, Princeton, NJ (1977).
3. Chopra, K.L. and Das, S.R., *Thin Film Solar Cells*, Plenum Press, New York (1983).
4. Hovel, H.J., in *Semiconductor and Semimetals*, **11** Academic Press, New York (1975).
5. Sittig, M. "Solar cells for photovoltaic generation of electricity", *Materials, Devices and Applications, Energy Technology Review*, **48**, Noyes Data Corp., Park Ridge, NJ (1979).
6. Aruchamy, A., Ed., *Photoelectrochemistry and Photovoltaics of Layered Materials*, Kluwer Academic Publishers, Dordrecht/Boston/London (1992).
7. Levy, F., Ed., *Intercalated Layered Materials*, D. Reidel Publishing Company, Dordrecht/Holland/Boston - USA (1979).
8. Wilson, J.A. and Yoffe, A.D. "The transition metal dichalcogenides, discussion and interpretation of the observed optical, electrical and structural properties", *Adv. Phys.*, **18**, pp 193-335 (1969).
9. Lee, P.A., Ed., *Optical and Electrical Properties of Layered Semiconductors*, D. Reidel Publ. Company, Dordrecht, Holland / Boston, USA (1976).
10. Prasad, G. and Srivastava, O.N. "The high efficiency (17.1%) WSe_2 photoelectrochemical solar cells", *J. Phys. D: Appl. Phys.*, **21**, pp 1028-1030 (1988).
11. Campet, G., Azaiez, C., Levy, F., Bourezc, H. and Claverie, J. "A 22% efficient semiconductor/liquid junction solar cell - The photoelectrochemical behavior of n-WSe_2 electrodes in the presence of I2/ I aqueous electrolyte", *Active and Passive Elec. Comp.*, **13**, pp 33-43 (1998).
12. Loferski, J.J. "Theoretical considerations governing the choice of the optimum semiconductor for photovoltaic solar energy conversion", *J. Appl. Phys.*, **27**, pp 777 -784 (1956).
13. Kam, K.K., Chang, C.L. and Lynch, D.W. "Fundamental absorption edges and indirect band gaps in $W_{1-x}Mo_xSe_2$ $(0 \leq x \leq 1)$", *J. Phys. C*, **17**, pp 4031-4040 (1984).
14. Baglio, J.A., Calabrese, G.S., Harrison, D.J., Kamieniecki, E., Ricco, A.J., Wrighton, M.S. and Zoski, G.D. "Electrochemical characterization of p-type semiconducting tungsten disulphide photocathodes: Efficient photoreduction processes at semiconductor/liquid electrolyte interfaces", *J. Am. Chem. Soc.*, **105**, pp 2246-2256 (1983).
15. Pankove, J.I., *Optical Processes in Semiconductors*, Dover Publ. Inc., New York (1975).
16. Vlachos, S.V., Lambros, A.P., Thanailakis, A. and Economou, N.A. "Anisotropic indirect absorption edge in GeSe", *Phys. Stat. Sol. (b)*, **76**, pp 727-735 (1976).
17. Elkorashy, A.M. "Indirect forbidden fundamental absorption edge in Germanium selenide single crystals", *Phys. Stat. Sol. (b)*, **135**, pp 707-713 (1986).
18. Elkorashy, A.M. "Optical absorption in tin monoselenide single crystal", *J. Phys. Chem. Solids*, **47**, pp 497-500 (1986).
19. Lee, P.A., Said, G., Davis, R. and Lim, T.H. "On the optical properties of some layer compounds", *J. Phys. Chem. Solids*, **30**, pp 2719-2729 (1969).
20. Goldberg, A.M., Beal, A.R., Levy, F.A. and Davis, E.A. "The low energy absorption edge in 2H-MoS_2 and 2H-$MoSe_2$", *Philos. Mag.*, **32**, pp 367-378 (1975).
21. Elkorashy, A.M. "The indirect forbidden fundainental absorption edge in single-crystal Germanium sulphide", *J. Phys. C: Solid State Phys.*, **21**, pp 2595-2607 (1988).
22. Koshkin, V.M., Karas, V.R. and Galchienestskii, L.P. "A method for the analysis of the optical absorption edge of semiconductors and applications to the absorption in In_2Te_3", *Fiz. Tekh. Poluprovobnikov*, **3**, pp 14172-14175 (1970).

23. Kam, K.K. and Parkinson, B.J. "Detailed photocurrent spectroscopy of the semiconducting group VI transition metal dichalcogenides", *J. Phys. Chem. Solids*, **86**, pp 463-467 (1982).

24. Srivastava, S.K. and Avasthi, B.N. "Layer type tungsten dichalcogenide compounds: Their preparation structure, properties and uses", *J. Mat. Sci.*, **20**, pp 3801-3815 (1985).

25. Agarwal, M.K., Rao, V.V. and Pathak, V.M. "Growth of n-type and p-type WSe_2 crystals using $SeCl_4$ transporter and their characterisation", *J. Cryst. Growth*, **97**, pp 675-679 (1989).

26. Kautek, W., Gerischer, H. and Tributsch, H. "The role of carrier diffusion and indirect optical transitions in the photoelectrochemical behavior of layer type-band semiconductors", *J. Electrochem. Soc.*, **127**, pp 2471-2478 (1980).

27. Kautek, W. and Gerischer, H. "Photoelectrochemical reactions and formation of inversion layers at n-type MoS_{2-}, $MoSe_2$, and WSe_{2-} electrodes in aquatic solvents", *Ber. Bunsenges Phys. Chem.*, **84**, pp 645-653 (1980).

28. Lewerenz, H.J., Ferris, S.D., Doherty, C.J. and Leamy, H.J. "Charge collection microscopy on p-WSe_2: Recombination sited and minority carrier diffusion length", *J. Electrochem. Soc.*, **129**, pp 418-423 (1982).

29. Agarwal, M.K., Vashi, M.N. and Jani, A.R. "Growth and characterization of the layer compounds in the series WS_xSe_{2-x}", *J. Cryst. Growth*, **71**, pp 415-420 (1985).

30. Anneda, A., Fortin, E. and Raga, F. "Optical spectra in WSe_2", *Can. J. Phys.*, **57**, pp 368-374 (1979).

31. Cabrera, C.R. and Abruna, H.D. "Synthesis and photoelectrochemistry of polycrystalline thin films of *p*-WSe_2, *p*-WS_2 and p-$MoSe_2$", *J. Electrochem. Soc.*, **135**, pp 1436-1442 (1988).

32. Chandra, S. and Sahu, S.N. "Electrodeposited tungsten selenide films", *Phys. Stat. Sol.(a)*, **89**, pp 321-331 (1985).

33. Baglio, J.A., Calabrese, G.S., Kamieniecki, E., Kershaw, R., Kubiak, C.P., Ricco, J., Wold, A., Wright, M.S. and Zoski, G.D. "Characterisation of n-type semiconducting tungsten disulphide photoanodes in aqueous and nonaqueous electrolyte solutions", *Electrochem. Soc.*, **129**, pp 1461-1472 (1982).

34. Donay, V. and Gorochov, O., *J. de Chimie. Physique*, **83**, p 4 (1986).

35. Van Vechten, J.A. and Bergstresser, T.K. "Electronic structures of semiconductor alloys", *Phys. Rev. B*, **1**, pp 3351-3355 (1970).